

# Effective equation for two coupled oscillators: towards a global view of metamorphoses of the amplitude profiles

Jan Kyzioł, Andrzej Okniński  
Politechnika Świętokrzyska, Al. 1000-lecia PP 7,  
25-314 Kielce, Poland

November 2, 2021

## Abstract

Dynamics of nonlinear coupled driven oscillators is investigated. Recently, we have demonstrated that the amplitude profiles – dependence of the amplitude  $A$  on frequency  $\Omega$  of the driving force, computed by asymptotic methods in implicit form as  $F(A, \Omega) = 0$ , permit prediction of metamorphoses of dynamics which occur at singular points of the implicit curve  $F(A, \Omega) = 0$ . In the present study we strive at a global view of singular points of the amplitude profiles computing bifurcation sets, i.e. sets containing all points in the parameter space for which the amplitude profile has a singular point.

## 1 Introduction

In this work we continue our investigation of coupled oscillators, see [1] and references therein. Coupled oscillators play important role in many scientific fields, e.g. neuroscience, chemistry, electronics, and mechanics, see [2–14] and references therein. A classic example is a dynamic vibration absorber, consisting of a mass  $m_2$ , attached to the primary vibrating system of mass  $m_1$  [15, 16] and described by equations:

$$\left. \begin{aligned} m_1 \ddot{x}_1 - V_1(\dot{x}_1) - R_1(x_1) + V_2(\dot{x}_2 - \dot{x}_1) + R_2(x_2 - x_1) &= f(t) \\ m_2 \ddot{x}_2 - V_2(\dot{x}_2 - \dot{x}_1) - R_2(x_2 - x_1) &= 0 \end{aligned} \right\} \quad (1)$$

where  $f(t) = f \cos(\omega t)$ ,  $V_1$ ,  $R_1$  and  $V_2$ ,  $R_2$  represent (nonlinear) force of internal friction and (nonlinear) elastic restoring force for mass  $m_1$  and mass  $m_2$ , respectively, see Fig. 1.

After making a simplifying assumption:

$$R_1(x_1) = -\alpha_1 x_1, \quad V_1(\dot{x}_1) = -\nu_1 \dot{x}_1, \quad (2)$$

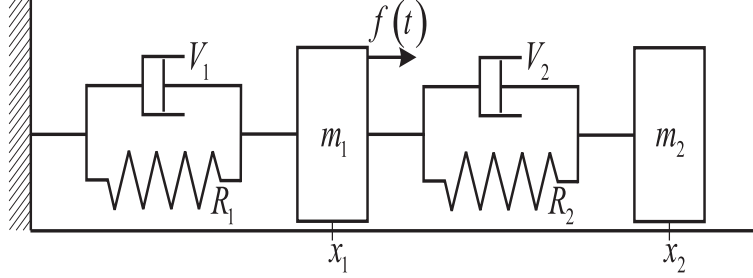


Figure 1: Dynamic vibration absorber. Definitions of  $R_1$ ,  $V_1$ ,  $R_2$ ,  $V_2$  adopted in this work are given in Eqs. (2), (4).

we derived approximate second-order effective equation and computed nonlinear resonances  $A(\omega) \cos(\omega t + \varphi)$  in implicit form  $F(A, \omega; c_1, c_2, \dots) = 0$  applying the Krylov-Bogoliubov-Mitropolsky (KBM) method [17] where  $c_1, c_2, \dots$  are parameters [18]. As explained in Section 3 and demonstrated in our earlier papers bifurcations occur at singular points of the amplitude equation  $F(A, \omega) = 0$ . In this work we attempt to find a global picture of singular points of the amplitude equation in the case of the effective equation, extending our results obtained for the van der Pol-Duffing equation [19].

The paper is organized as follows. In the next Section the effective equation and the amplitude profile of the nonlinear resonance, obtained in Ref. [18], are described. In Section 3 singular points of the amplitude equation are defined and their relation to bifurcation of dynamics is explained. In Section 4 theory of algebraic curves is applied to compute the bifurcation set for the effective equation obtaining thus a global view of bifurcations. Plots of the bifurcation set and examples of singular points as well as corresponding bifurcations are presented in Section 5 and we summarize our results in the last Section.

## 2 Approximate effective equation and the Krylov-Bogoliubov-Mitropolsky amplitude profile

In new variables,  $x \equiv x_1$ ,  $y \equiv x_2 - x_1$ , we can eliminate variable  $x$  to obtain the following exact equation for relative motion [18, 20]:

$$\left( M \frac{d^2}{dt^2} + \nu_1 \frac{d}{dt} + \alpha_1 \right) (\mu \ddot{y} - V_2(\dot{y}) - R_2(y)) + \epsilon m_2 \left( \nu_1 \frac{d}{dt} + \alpha_1 \right) \ddot{y} = \hat{f}(t), \quad (3)$$

where  $\hat{f}(t) = m_2 \omega^2 f \cos(\omega t)$ ,  $M = m_1 + m_2$ ,  $\mu = m_1 m_2 / M$ ,  $\epsilon = m_2 / M$ .

In the present work we put:

$$R_2(y) = \alpha_2 y - \gamma_2 y^3, \quad V_2(\dot{y}) = -\nu_2 \dot{y}, \quad (4)$$

and assume that  $\epsilon m_2, \nu_1, \alpha_1$  are small so that the term proportional to  $\epsilon m_2$  can be neglected.

Introducing nondimensional time  $\tau$  and rescaling variable  $y$ :

$$\tau = t\bar{\omega}, \quad \bar{\omega} = \sqrt{\frac{\alpha_2}{\mu}}, \quad z = y\sqrt{\frac{\gamma_2}{\alpha_2}}, \quad (5)$$

we get the approximate effective equation [18]:

$$\frac{d^2 z}{d\tau^2} + h \frac{dz}{d\tau} - z + z^3 = -\gamma \frac{\Omega^2}{\sqrt{(\Omega^2 - a)^2 + H^2 \Omega^2}} \cos(\Omega\tau), \quad (6)$$

with  $\gamma \equiv G \frac{\kappa}{\kappa+1}$  and where nondimensional constants are given by:

$$h = \frac{\nu_2}{\mu\bar{\omega}}, \quad H = \frac{\nu_1}{M\bar{\omega}}, \quad \Omega = \frac{\omega}{\bar{\omega}}, \quad G = \frac{1}{\alpha_2} \sqrt{\frac{\gamma_2}{\alpha_2}} f, \quad \kappa = \frac{m_2}{m_1}, \quad a = \frac{\alpha_1 \mu}{\alpha_2 M}. \quad (7)$$

We applied the Krylov-Bogoliubov-Mitropolsky (KBM) perturbation approach [17] to the effective equation (6) obtaining the following implicit amplitude equation  $F(A, \Omega) = 0$  for the 1 : 1 resonance [18]:

$$A = \frac{\gamma \Omega^2}{\sqrt{\left(h^2 \Omega^2 + \left(1 + \Omega^2 - \frac{3}{4} A^2\right)^2\right) \left((\Omega^2 - a)^2 + H^2 \Omega^2\right)}}. \quad (8)$$

After a smooth change of variables,  $X \equiv \Omega^2, Y \equiv A^2$ , Eq. (8) can be written as:

$$L(X, Y) = \left(h^2 X + \left(1 + X - \frac{3}{4} Y\right)^2\right) \left((X - a)^2 + H^2 X\right) Y - \gamma^2 X^2 = 0. \quad (9)$$

### 3 Singular points of the amplitude profile and bifurcations of dynamics

Let us consider a one degree of freedom dynamical system described by a non-linear, nonautonomous in general, ordinary differential equation of form:

$$\frac{d^2 y}{dt^2} + \omega^2 y = \epsilon f\left(y, \frac{dy}{dt}, t\right), \quad (10)$$

where  $\epsilon$  is a small parameter and  $f$  is a periodic function of time with period  $T = \frac{2\pi}{\Omega}$ .

Applying the KBM method, or another asymptotic procedure, we can find an approximate solution, the so-called 1 : 1 nonlinear resonance, of form:

$$y(t) = A \cos(\Omega t + \varphi) + \epsilon y_1(t) + \dots \quad (11)$$

where unknown amplitude  $A$  and unknown frequency  $\Omega$  fulfill the amplitude equation:

$$F(A, \Omega; \underline{c}) = 0, \quad (12)$$

where  $\underline{c} = (c_1, c_2, \dots, c_n)$  are parameters. Equation (12) defines an implicit function – a two-dimensional planar curve - the amplitude profile. The form of this curve, as well as stability of the solution (11), determine (approximately) dynamics of the system. In most cases the approximation (11), (12) provides a good insight into dependence of the dynamics on parameters.

It thus follows that qualitative changes of shape of the amplitude profile (12), referred henceforth as metamorphoses, induced by smooth changes of control parameters  $\underline{c}$ , lead to qualitative changes of dynamics (bifurcations) because dependence of the amplitude  $A$  on frequency  $\Omega$  changes qualitatively.

Stability of the solution (11) is very important since it determines which parts of the implicit curve (12) show up in actual dynamics. Assume, for the sake of an example, that for fixed parameters  $\underline{c}$  the curve  $A(\Omega)$  has several branches in the interval  $\Omega \in (\Omega_1, \Omega_2)$ . Typically, only some branches (or parts of these) are stable in this interval. The shape of the amplitude profile (12) (the stable part) can be displayed by a bifurcation diagram, computed by numerical integration of the equation (10) in the interval  $\Omega \in (\Omega_1, \Omega_2)$  for fixed parameters  $\underline{c}$ . Bifurcation diagrams, computed for slowly changing parameters  $\underline{c}$ , can thus reveal metamorphoses of the amplitude profiles.

According to the differential geometry of curves [21, 22] an implicit curve changes its form at singular points which fulfill the following equations:

$$F(A, \Omega; \underline{c}) = 0, \quad (13a)$$

$$\frac{\partial F(A, \Omega; \underline{c})}{\partial A} = 0, \quad (13b)$$

$$\frac{\partial F(A, \Omega; \underline{c})}{\partial \Omega} = 0. \quad (13c)$$

Solutions  $A_*$ ,  $\Omega_*$ ,  $\underline{c}_*$  of Eqs. (13) are indeed special (singular). Equation (13b) implies that a function  $A = g(\Omega)$  has no first derivative at  $\Omega = \Omega_*$  while Eq. (13c) means that a function  $\Omega = f(A)$  is not differentiable at  $A = A_*$  [21, 22].

These conditions become more transparent when  $F(A, \Omega; \underline{c})$  is a polynomial in variables  $A$ ,  $\Omega$ . In this case Eqs. (13a), (13b) mean that a polynomial  $F(A, \Omega_*, \underline{c}_*) = a_N A^N + \dots + a_1 A + a_0 = 0$  has multiple solutions (accordingly, a function  $A = g(\Omega)$  is not single-valued at  $\Omega = \Omega_*$ ) while it follows from equations (13a), (13c) that a polynomial  $F(A_*, \Omega, \underline{c}_*) = b_M \Omega^M + \dots + b_1 \Omega + b_0 = 0$  has multiple solutions (and a function  $\Omega = f(A)$  is not single-valued at  $A = A_*$ ). Accordingly,  $A_*$ ,  $\Omega_*$ ,  $\underline{c}_*$  is a multiple solution of Eqs. (13).

Assume that a solution  $(A_*, \Omega_*)$  of Eqs. (13) exists for  $\underline{c} = \underline{c}_*$  and there are no other solutions in some neighbourhood of  $\underline{c}_*$ . Consider a curve  $\lambda$  in the parameter space containing the point  $\underline{c}_*$ . Then, when the curve  $\lambda$  passes through the point  $\underline{c}_*$ , the implicit function (12) changes its shape. We shall refer to such a change as metamorphosis. This change depends on the nature of a singular

point. Two simplest examples of singular points are isolated point and self-intersection. In an isolated point a new branch of solution (stable or unstable) is born or disappears, while in a self-intersection a branch (stable or unstable) becomes disconnected or two branches are joined. In this work we compute the bifurcation set – the set in the parameter space containing all singular points of the amplitude profile, see Ref. [19] where the bifurcation set was computed for the van der Pol-Duffing oscillator [19].

The approach outlined in this Section can be generalized for  $m : n$  resonances [23] and for a system of coupled ordinary differential equations (1) [24]. Investigation of changes of shape of an amplitude profile induced by change of parameters was carried out in [25] for the Duffing equation. This is, however, a non-singular case [26] and thus only Eq. (13a) and equivalent of Eq. (13b) were used. The idea to use Implicit Function Theorem to "define and find different branches intersecting at singular points" of amplitude profiles was proposed in [27].

## 4 Global view of metamorphoses of the amplitude profiles

### 4.1 Singular points

We shall investigate singular points of the amplitude equation (9) because bifurcations occur at these points, cf. Section 3. Singular points of algebraic curve  $L(X, Y; a, h, H, \gamma) = 0$  are given by equations analogous to (13):

$$L = 0, \quad (14a)$$

$$\frac{\partial L}{\partial X} = 0, \quad (14b)$$

$$\frac{\partial L}{\partial Y} = 0. \quad (14c)$$

Equation (14c) factorizes as:

$$\frac{\partial L}{\partial Y} = \frac{1}{16} (H^2 X + X^2 - 2Xa + a^2) \times (16X^2 - 48XY + 16Xh^2 + 32X + 27Y^2 - 48Y + 16) = 0. \quad (15)$$

It follows that the condition  $H^2 X + X^2 - 2Xa + a^2 = 0$  does not lead to physical solutions [26], therefore instead of (14c) we consider a simpler equation:

$$M(X, Y; h) \equiv 16X^2 - 48XY + 16Xh^2 + 32X + 27Y^2 - 48Y + 16 = 0. \quad (16)$$

Now we notice that the equation (16) reduces to linear relations between  $X$  and  $Y$  for two physical values of  $h$ :  $h_0^{(1)} = \sqrt{\frac{4}{3}}$ ,  $h_0^{(2)} = 0$ . Indeed, we have:

$$M(X, Y; h_0^{(1)}) = \frac{1}{3} (4X - 9Y + 12) (12X - 9Y + 4) = 0, \quad (17a)$$

$$M(X, Y; h_0^{(2)}) = (4X - 9Y + 4) (4X - 3Y + 4) = 0. \quad (17b)$$

## 4.2 Bifurcation set

It follows from general theory of implicit functions that in a singular point there are multiple solutions of equation (9). We shall use this property to compute parameters values for which the amplitude profile defined by equation (9) has singular points. We shall refer to such set in the parameter space as the bifurcation set, see Ref. [25] where this term was used in the context of multiple solutions of the amplitude equation for the Duffing equation (albeit in the non-singular case).

To define a singular point we can use equations (14a), (14b) and an alternative to condition (14c) which excludes existence of the single-valued function  $Y = g(X)$ . We thus solve Eqs. (14a), (14b) obtaining equation  $f(X) = 0$  for a function  $Y = f(X)$  and then demand that there are multiple solutions of this equation (alternatively, we could have solved Eqs. (14a), (14c)).

Solution of Eqs. (14a), (14b), with  $L(X, Y; a, h, H, \gamma)$  given by Eq. (9) can be written as the following equation for  $X$ :

$$f(X) = a_8 X^8 + a_7 X^7 + a_6 X^6 + a_5 X^5 + a_4 X^4 + a_3 X^3 + a_2 X^2 + a_1 X + a_0 = 0, \quad (18)$$

with coefficients  $a_0, a_1, \dots, a_8$  given in the A.

Necessary and sufficient condition for a polynomial to have multiple roots is that its discriminant  $\Delta$  vanishes [28], see also lecture notes [29]. Discriminant  $\Delta$  can be computed as a resultant of a polynomial  $f(X)$  and its derivative  $f'$ , with a suitable normalizing factor.

Resultant  $R(f, g)$  of two polynomials,  $f(X) = a_n X^n + \dots + a_1 X + a_0$ ,  $g(X) = b_m X^m + \dots + b_1 X + b_0$ , is given by determinant of the  $(m+n) \times (m+n)$  Sylvester matrix:

$$R(f, g) = \det \begin{pmatrix} a_n & a_{n-1} & a_{n-2} & \dots & 0 & 0 & 0 \\ 0 & a_n & a_{n-1} & \dots & 0 & 0 & 0 \\ \vdots & \vdots & \vdots & & \vdots & \vdots & \vdots \\ 0 & 0 & 0 & \dots & a_1 & a_0 & 0 \\ 0 & 0 & 0 & \dots & a_2 & a_1 & a_0 \\ b_m & b_{m-1} & b_{m-2} & \dots & 0 & 0 & 0 \\ 0 & b_m & b_{m-1} & \dots & 0 & 0 & 0 \\ \vdots & \vdots & \vdots & & \vdots & \vdots & \vdots \\ 0 & 0 & 0 & \dots & b_1 & b_0 & 0 \\ 0 & 0 & 0 & \dots & b_2 & b_1 & b_0 \end{pmatrix}, \quad (19)$$

see, for example, Eq. (1) in [29]. Polynomials  $f$  and  $g$  have a common root if and only if  $R(f, g) = 0$ .

Therefore, the bifurcation set  $\mathcal{M}$  is given by the following equations:

$$(a, h, H, \gamma) \in \mathcal{M} : \quad R(f, f') = 0, \quad (20)$$

where  $R(f, f')$  is defined in (19) as determinant of the  $15 \times 15$  Sylvester matrix with  $g = f'$ . The polynomial  $f(X)$  has been defined in (18), with coefficients

$a_0, a_1, \dots, a_8$  given in the A and

$$f'(X) = 8a_8X^7 + 7a_7X^6 + \dots + 2a_2X + a_1 \equiv b_7X^7 + b_6X^6 + \dots + b_1X + b_0. \quad (21)$$

Obviously,  $R(f, f')$  depends on the parameters  $a, h, H, \gamma$  and will be also denoted as  $R(f, f')(a, h, H, \gamma)$ .

### 4.3 Plots of the bifurcation set

The equation  $R(f, f') = 0$  (20) leads to a high-order polynomial in variables  $a, h, H, \gamma$ . We were able, however, to plot 3D sections of the bifurcation set,  $R(f, f')(a, h, H, \gamma) = 0$ , for fixed values of  $h = h_0$  using the High Performance Computing Cluster (HPCC) at Politechnika Świętokrzyska.

The computations are much easier for  $h_0^{(1)} = \sqrt{\frac{4}{3}}$  and  $h_0^{(2)} = 0$  since then the polynomial (18) factorizes into a product of two polynomials – note that for these values of  $h$  the equation (16) factorizes, see Eqs. (17a), (17b). More exactly, for  $h_0^{(1)} = \sqrt{\frac{4}{3}}$

$$\begin{aligned} f(X) &= f_1(X) f_2(X), \\ f_1(X) &= b_4X^4 + b_3X^3 + b_2X^2 + b_1X + b_0, \\ f_2(X) &= c_4X^4 + c_3X^3 + c_2X^2 + c_1X + c_0, \end{aligned} \quad (22)$$

where

$$\left. \begin{aligned} b_4 &= 144, \quad b_3 = -288a + 144H^2 + 96 \\ b_2 &= 144a^2 - 192a + 96H^2 - 81\gamma^2 + 16 \\ b_1 &= 96a^2 - 32a + 16H^2, \quad b_0 = 16a \end{aligned} \right\}, \quad (23)$$

$$\left. \begin{aligned} c_4 &= 16, \quad c_3 = -32a + 16H^2 + 96 \\ c_2 &= 16a^2 - 192a + 96H^2 + 144 \\ c_1 &= 96a^2 - 288a + 144H^2 - 81\gamma^2, \quad c_0 = 144a^2 \end{aligned} \right\}, \quad (24)$$

while for  $h_0^{(2)} = 0$  we have:

$$\begin{aligned} f(X) &= -3\gamma^2 X g(X), \\ g(X) &= d_5X^5 + d_4X^4 + d_3X^3 + d_2X^2 + d_1X + d_0, \end{aligned} \quad (25)$$

where

$$\left. \begin{aligned} d_5 &= 16, \quad d_4 = 16H^2 - 32a + 48 \\ d_3 &= 48 + 16a^2 - 96a + 48H^2 \\ d_2 &= 48H^2 + 48a^2 - 81\gamma^2 + 16 - 96a \\ d_1 &= -32a + 48a^2 + 16H^2, \quad d_0 = 16a^2 \end{aligned} \right\}. \quad (26)$$

Discriminant of a quartic polynomial  $f(x) = ax^4 + bx^3 + cx^2 + dx + e$  is:

$$\begin{aligned} \Delta &= 256a^3e^3 - 192a^2bde^2 - 128a^2c^2e^2 + 144a^2cd^2e - 27a^2d^4 \\ &+ 144ab^2ce^2 - 6ab^2d^2e - 80abc^2de + 18abcd^3 + 16ac^4e \\ &- 4ac^3d^2 - 27b^4e^2 + 18b^3cde - 4b^3d^3 - 4b^2c^3e + b^2c^2d^2 \end{aligned} \quad (27)$$

Therefore, the bifurcation set for  $h_0^{(1)} = 0$  consists of three subsets:  $\Delta_1(a, H, \gamma) = 0$ ,  $\Delta_2(a, H, \gamma) = 0$  where  $\Delta_1, \Delta_2$  are discriminants of polynomials  $f_1, f_2$ , respectively, and  $R(f_1, f_2) = 0$  where the resultant  $R(f_1, f_2)$  reads:

$$R(f_1, f_2) = \det \begin{pmatrix} b_4 & b_3 & b_2 & b_1 & b_0 & 0 & 0 & 0 \\ 0 & b_4 & b_3 & b_2 & b_1 & b_0 & 0 & 0 \\ 0 & 0 & b_4 & b_3 & b_2 & b_1 & b_0 & 0 \\ 0 & 0 & 0 & b_4 & b_3 & b_2 & b_1 & b_0 \\ c_4 & c_3 & c_2 & c_1 & c_0 & 0 & 0 & 0 \\ 0 & c_4 & c_3 & c_2 & c_1 & c_0 & 0 & 0 \\ 0 & 0 & c_4 & c_3 & c_2 & c_1 & c_0 & 0 \\ 0 & 0 & 0 & c_4 & c_3 & c_2 & c_1 & c_0 \end{pmatrix} \quad (28)$$

$$= 2^{12} 3^8 \gamma^4 a^2 (256a^2 - 512a + 256H^2 - 81\gamma^2 + 256)^3$$

These three subsets are plotted in Fig. (2). Discriminant of the quintic polynomial is more complicated:

$$\Delta = a_5^{-1} \det \begin{pmatrix} a_5 & a_4 & a_3 & a_2 & a_1 & a_0 & 0 & 0 & 0 \\ 0 & a_5 & a_4 & a_3 & a_2 & a_1 & a_0 & 0 & 0 \\ 0 & 0 & a_5 & a_4 & a_3 & a_2 & a_1 & a_0 & 0 \\ 0 & 0 & 0 & a_5 & a_4 & a_3 & a_2 & a_1 & a_0 \\ 5a_5 & 4a_4 & 3a_3 & 2a_2 & a_1 & 0 & 0 & 0 & 0 \\ 0 & 5a_5 & 4a_4 & 3a_3 & 2a_2 & a_1 & 0 & 0 & 0 \\ 0 & 0 & 5a_5 & 4a_4 & 3a_3 & 2a_2 & a_1 & 0 & 0 \\ 0 & 0 & 0 & 5a_5 & 4a_4 & 3a_3 & 2a_2 & a_1 & 0 \\ 0 & 0 & 0 & 0 & 5a_5 & 4a_4 & 3a_3 & 2a_2 & a_1 \end{pmatrix}, \quad (29)$$

see Eq. (1.36) in Chapter 12 in [28] for explicit formula.

The bifurcation set  $\Delta(a, H, \gamma) = 0$ , where  $\Delta$  is discriminant (29) of polynomial  $g(X)$ , see Eq. (25), is plotted in Fig. 3.

Moreover, for  $h_0^{(1)} = \sqrt{\frac{4}{3}}$  we were able to compute degenerate singular points, i.e. fulfilling Eqs. (14) and additional condition:

$$\frac{\partial^2 L}{\partial X^2} \frac{\partial^2 L}{\partial Y^2} - \left( \frac{\partial^2 L}{\partial X \partial Y} \right)^2 = 0, \quad (30)$$

which implies that determinant of the Hesse matrix vanishes. The physical solution reads:

$$\left. \begin{aligned} h_* &= h_0^{(1)} = \sqrt{\frac{4}{3}}, \quad H_* = \frac{1}{32} \sqrt{-2048 + 162\gamma^2 + 64\sqrt{1024 + 162\gamma^2}}, \\ a_* &= -1 + \sqrt{4 + H_*^2}, \quad \gamma - \text{arbitrary}, \quad X_* = 1, \quad Y_* = \frac{16}{9}. \end{aligned} \right\} \quad (31)$$

Let us note that these parameters  $a_*, H_*, \gamma$  are also a solution of equations:

$$\Delta_1(a, H, \gamma) = 0, \quad \Delta_2(a, H, \gamma) = 0, \quad R(f_1, f_2) = 0, \quad (32)$$

hence three surfaces in Fig. (2) are tangent along line  $(a_*, H_*, \gamma)$ .



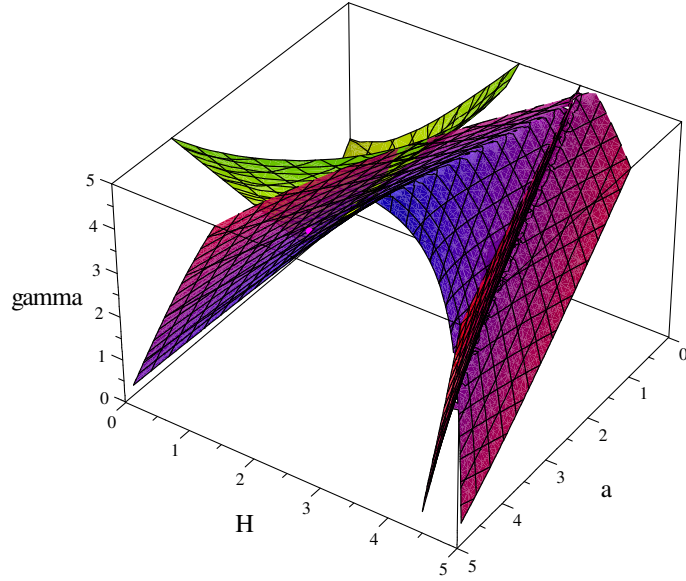
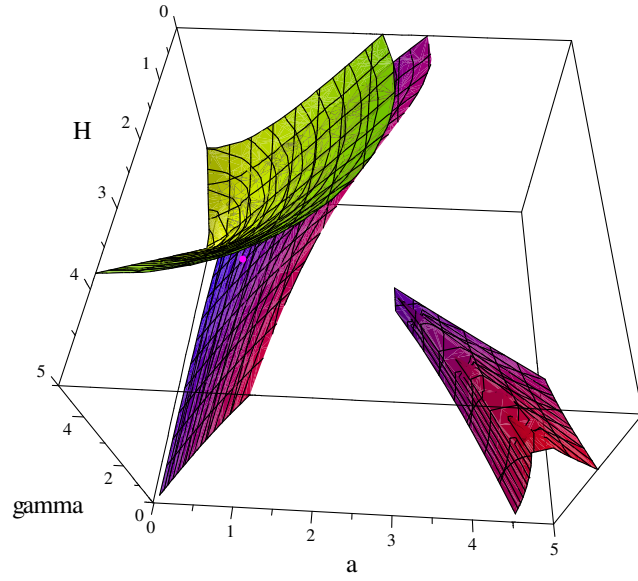


Figure 2: The bifurcation subsets  $\left(h_0^{(1)} = \sqrt{\frac{4}{3}}\right)$ :  $\Delta_1(a, H, \gamma) = 0$  blue-red and  $R(f_1, f_2) = 0$  yellow-green (top) and  $\Delta_2(a, H, \gamma) = 0$  blue-red and  $R(f_1, f_2) = 0$  yellow-green (bottom). Magenta dots mark singular points described in Section 5.

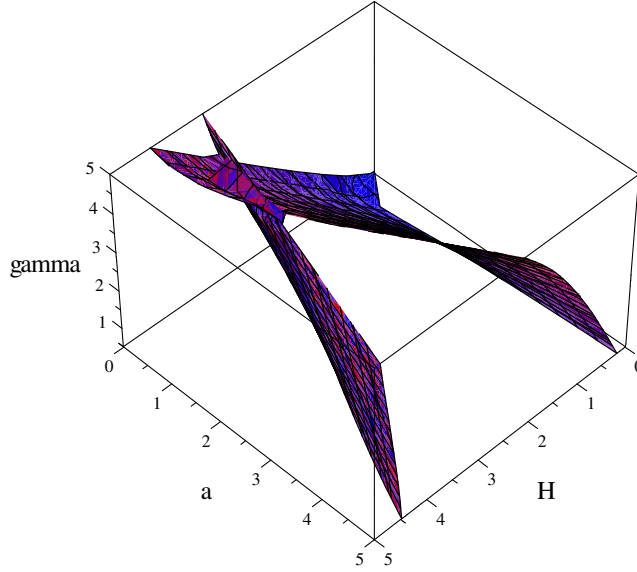


Figure 3: The bifurcation set:  $\Delta(a, H, \gamma) = 0, h_0^{(2)} = 0$ .

We shall now determine the form of the amplitude profile  $F(A, \Omega) = 0$  in the case of a degenerate singular point and for two singular points in its vicinity in the parameter space. Let  $h_* = \sqrt{\frac{4}{3}}$ . Then, we have from Eq. (31)  $a_* = 1.193171, H_* = 0.9, \gamma_* = 1.636439$ . The amplitude profile in the case of degenerate singular point has a cusp, see black line in Fig. 4.

There are also two singular non-degenerate points shown in Fig. 4: self intersection (red line) and isolated point (blue-green). The parameters were chosen as  $h = \sqrt{\frac{4}{3}}, H = 0.9, \gamma = 2$ . Solving equation  $\Delta_1 = 0$  we get  $a = 2.199923$  – it is an isolated point, while  $\Delta_2 = 0$  yields  $a = 2.156818$  – a self-intersection, see also magenta dots in Fig. 2.

Sections of the bifurcation set displayed in Figs. 2, 3 has been computed for  $h_0^{(1)} = \sqrt{\frac{4}{3}}, h_0^{(2)} = 0$ , respectively, since then the polynomial (18) factorizes and computations are simpler. For the sake of comparison, we have also computed and plotted the bifurcation set for  $h_0^{(3)} = 1$ , using the HPCC, see Fig. 5.

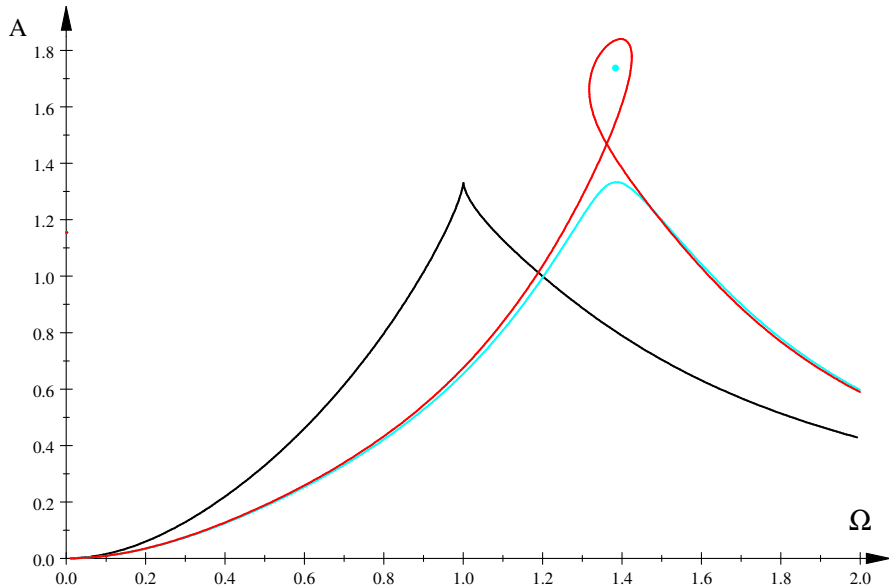


Figure 4: The amplitude profiles:  $a = a_*$ ,  $h = h_*$ ,  $H = H_*$ ,  $\gamma = \gamma_*$  (black, degenerate singular),  $h = \sqrt{\frac{4}{3}}$ ,  $H = 0.9$ ,  $\gamma = 2$ ,  $a_1 = 2.199\,923$  (blue-green, isolated point),  $a_2 = 2.156\,818$  (red, self-intersection).

## 5 Examples of bifurcations at singular points of the amplitude profile

We shall demonstrate that knowledge of singular points of the amplitude profiles  $F(A, \Omega) = 0$ , computed by application of the KBM method and defined implicitly in Eq. (8) or (9), permits prediction of metamorphoses of dynamics.

Global views of singular points are displayed in Figs. 2, 3, 5, showing  $\mathcal{M}(a, h_0, H, \gamma)$  – sections of the bifurcation set defined in Eq. (20). More exactly, for each point  $(a, h_0, H, \gamma) \in \mathcal{M}$  the amplitude profile  $F(A, \Omega; a, h_0, H, \gamma) = 0$  has a singular point.

Consider, for example, the case  $h_0^{(1)} = \sqrt{\frac{4}{3}}$ . It follows from Figs. (2), (4) that in the neighbourhood of a degenerate singular points  $(a_*, h_*, H_*, \gamma)$  there are two kinds of singular points: isolated points and self-intersections. In the neighbourhood of the first singular point  $(a, h, H, \gamma) = (2.156\,818, h_0^{(1)}, 0.9, 2)$  the amplitude profiles are shown in Fig. 6:

Bifurcation diagrams [30] show, indeed, metamorphosis of dynamics, see Fig. 7:

Fig. 7 shows clearly which parts of the amplitude profiles  $F(A, \Omega) = 0$  shown in Fig. 6 are stable. Please note that in the computed bifurcation diagrams only

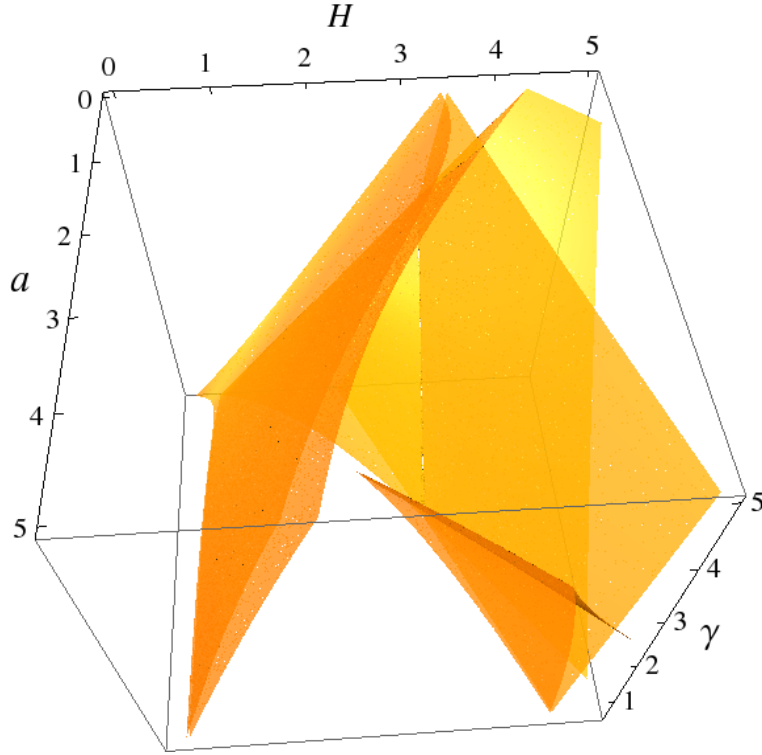


Figure 5: The bifurcation set,  $h_0^{(3)} = 1$ .

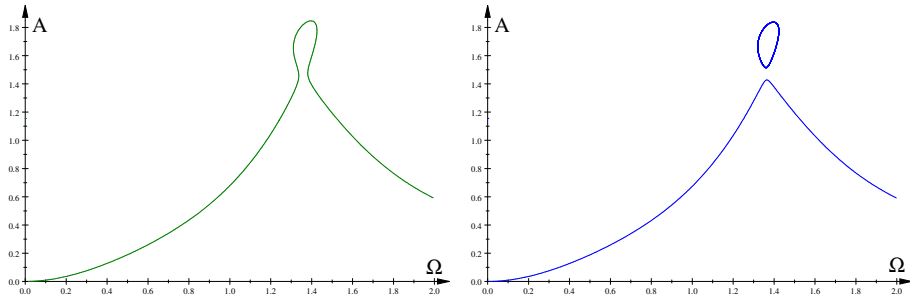


Figure 6: The amplitude profiles:  $h = h_0^{(1)}$ ,  $H = 0.9$ ,  $\gamma = 2$ ,  $a = 2.15$  (left, green),  $a = 2.16$  (right, blue).

stable solutions are displayed.

Near the second singular point  $(a, h, H, \gamma) = (2.199923, h_0^{(1)}, 0.9, 2)$  the amplitude profiles are shown in Fig. 8 and the corresponding bifurcation diagrams are displayed in Fig. 9. Figs. 8, 9 show metamorphosis of dynamics –

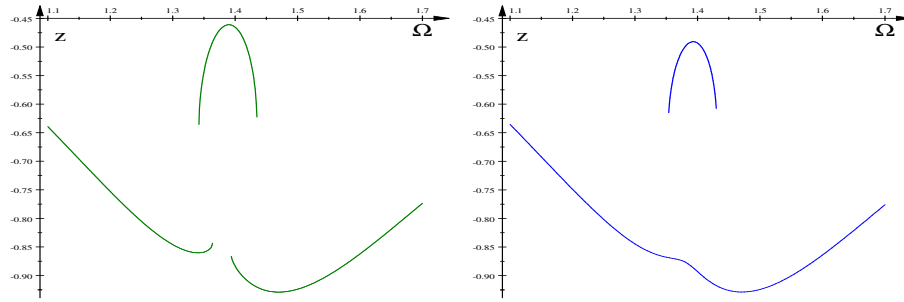


Figure 7: The bifurcation diagrams:  $h = h_0^{(1)}$ ,  $H = 0.9$ ,  $\gamma = 2$ ,  $a = 2.21$  (left, green),  $a = 2.22$  (right, blue).

disappearance of a branch of the solution.

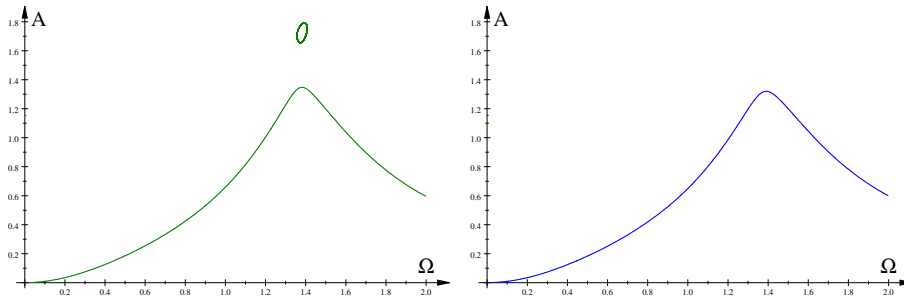


Figure 8: The amplitude profiles:  $h = h_0^{(1)}$ ,  $H = 0.9$ ,  $\gamma = 2$ ,  $a = 2.19$  (left, green),  $a = 2.21$  (right, blue).

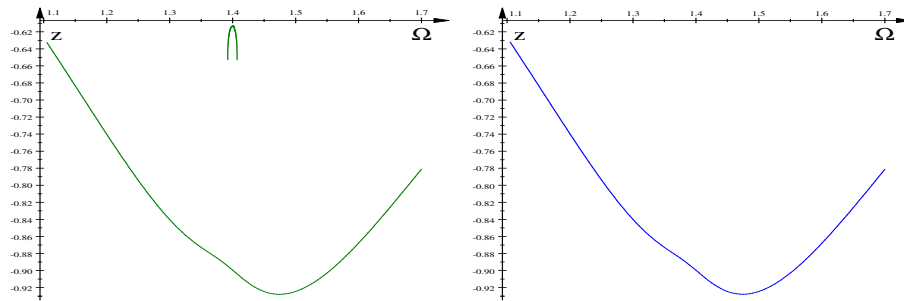


Figure 9: The bifurcation diagrams:  $h = h_0^{(1)}$ ,  $H = 0.9$ ,  $\gamma = 2$ ,  $a = 2.242$  (left, green),  $a = 2.243$  (right, blue).

## 6 Summary and discussion

In this work we have studied metamorphoses of amplitude profiles for the effective equation (6) which describes approximately dynamics of two coupled periodically driven oscillators. Our computations are based on the amplitude profile  $F(A, \Omega) = 0$  computed in [26] within the approximate KBM method. We have demonstrated in our earlier papers that the amplitude profiles  $F(A, \Omega) = 0$  computed by the KBM method permit prediction of metamorphoses of dynamics which occur at singular points.

In the present study we have strived at a global view of singular points of the amplitude profiles. We have derived equations for the bifurcation set, see Eqs. (20), (19), (18) and the A. The bifurcation set is thus a four-dimensional manifold  $\mathcal{M}$  containing all points  $(a, h, H, \gamma)$  for which the amplitude profile  $F(A, \Omega; a, h, H, \gamma) = 0$  is singular. Examples of plots of  $\mathcal{M}$  and the corresponding bifurcations are given in Sections 4.3 and 5, respectively.

### A Coefficients of the polynomial (18)

$$\begin{aligned}
 a_0 &= 64a^4h^2 \\
 a_1 &= 128h^4a^4 + 128H^2h^2a^2 - 48a^2\gamma^2 - 256a^3h^2 + 256a^4h^2 \\
 a_2 &= \left( \begin{array}{l} 64h^6a^4 + 384a^4h^2 + 256h^4a^4 + 96\gamma^2a + 64H^4h^2 + 384h^2a^2 \\ -144a^2\gamma^2 - 512h^4a^3 - 256H^2h^2a + 256h^4H^2a^2 + 512H^2h^2a^2 \\ -432\gamma^2h^2a^2 - 48\gamma^2H^2 - 1024a^3h^2 \end{array} \right) \\
 a_3 &= \left( \begin{array}{l} 128h^4a^4 - 256h^2a + 128h^2H^2 - 256h^6a^3 - 1024h^4a^3 \\ +256H^4h^2 - 432\gamma^2h^2a^2 - 144\gamma^2H^2 + 768H^2h^2a^2 + 1536h^2a^2 \\ -144a^2\gamma^2 + 864\gamma^2h^2a - 1536a^3h^2 + 768h^4a^2 + 243\gamma^4 \\ +256a^4h^2 - 48\gamma^2 + 288\gamma^2a - 512h^4aH^2 - 432\gamma^2h^2H^2 \\ -1024H^2h^2a + 128h^4H^4 + 512h^4H^2a^2 + 128h^6H^2a^2 \end{array} \right) \\
 a_4 &= \left( \begin{array}{l} 64h^2 + 288\gamma^2a - 144\gamma^2H^2 + 2304h^2a^2 - 1024h^2a + 512h^2H^2 \\ -432\gamma^2h^2 + 64a^4h^2 + 384h^6a^2 - 512h^4a + 1536h^4a^2 - 144\gamma^2 \\ -256h^6aH^2 + 864\gamma^2h^2a + 512H^2h^2a^2 - 432\gamma^2h^2H^2 - 1536H^2h^2a \\ -1024h^4aH^2 + 256h^4H^2a^2 + 64h^6H^4 - 512h^4a^3 + 256h^4H^2 \\ +256h^4H^4 - 1024a^3h^2 + 384H^4h^2 - 48a^2\gamma^2 \end{array} \right) \\
 a_5 &= \left( \begin{array}{l} 256H^4h^2 - 48\gamma^2H^2 + 128h^4 - 256a^3h^2 + 512h^4H^2 + 1536h^2a^2 \\ +768h^4a^2 - 1536h^2a - 432\gamma^2h^2 + 96\gamma^2a + 256h^2 - 1024h^4a \\ -144\gamma^2 - 256h^6a - 512h^4aH^2 - 1024H^2h^2a + 128h^6H^2 + 128h^4H^4 \\ +768h^2H^2 + 128H^2h^2a^2 \end{array} \right) \\
 a_6 &= \left( \begin{array}{l} 512h^2H^2 + 64h^6 + 384h^2a^2 - 48\gamma^2 - 512h^4a + 384h^2 \\ +64H^4h^2 - 1024h^2a - 256H^2h^2a + 256h^4 + 256h^4H^2 \end{array} \right) \\
 a_7 &= 128h^4 - 256h^2a + 256h^2 + 128h^2H^2 \\
 a_8 &= 64h^2
 \end{aligned}$$

## B Computational details

Nonlinear polynomial equations were solved numerically using the computational engine Maple 4.0 from the Scientific WorkPlace 4.0. Fig. 5 was plotted by the computational engine Mathematica 9.0 installed in the High Performance Computing Cluster at Politechnika Świętokrzyska (Kielce University of Technology). Other figures were plotted with the computational engine MuPAD 4.0 from Scientific WorkPlace 5.5. Curves shown in bifurcation diagrams in Figs. 7, 9 were computed by integrating numerically Eq. (6) running DYNAMICS, program written by Helena E. Nusse and James A. Yorke [30], and our own programs written in Pascal.

## References

- [1] J. Kyzioł, A. Okniński, Metamorphoses of resonance curves in systems of coupled oscillators: The case of degenerate singular points, *Int. J. Non-Linear Mechanics* **95**, 272–276 (2017).
- [2] G.M. Mahmoud, T. Bountis, The dynamics of systems of complex nonlinear oscillators: a review, *Int. J. Bifur. Chaos* **14** (2004) 3821-3846.
- [3] A. Pikovsky, M. Rosenblum, Dynamics of globally coupled oscillators: Progress and perspectives, *Chaos*, **25** (2015) 097616.
- [4] N.W. Schultheiss, A.A. Prinz, R.J. Butera, eds. *Phase response curves in neuroscience: theory, experiment, and analysis*. Springer A Science & Business Media, 2011.
- [5] N.M. Awal, D. Bullara, I.R. Epstein, The smallest chimera, Periodicity and chaos in a pair of coupled chemical oscillators, *Chaos* **29** (2019) 013131.
- [6] A.Z. Hajjaj, N. Jaber, S. Ilyas, F.K. Alfosail, M.I. Younis, Linear and nonlinear dynamics of micro- and nano-resonators: Review of recent advances, *Int. J. Non-Linear Mechanics*, 2019, March 2020, 103328, <https://doi.org/10.1016/j.ijnonlinmec.2019.103328>.
- [7] J. Kozłowski, U. Parlitz and W. Lauterborn, Bifurcation analysis of two coupled periodically driven Duffing oscillators, *Phys. Rev. E* **51** (1995) 1861-1867.
- [8] A. P. Kuznetsov, N. V. Stankevich and L. V Turukina, Coupled van der Pol-Duffing oscillators: phase dynamics and structure of synchronization tongues, *Physica D* **238** (2009) 1203-1215.
- [9] E. Perkins, B. Balachandran, Noise-enhanced response of nonlinear oscillators, *Procedia Iutam* **5** (2012) 59-68.

- [10] S. Sabarathinam, K. Thamilmaran, L. Borkowski, P. Perlikowski, P. Brzeski, A. Stefanski, T. Kapitaniak, Transient chaos in two coupled, dissipatively perturbed Hamiltonian Duffing oscillators, *Commun. Nonlinear Sci Numer. Simulat.* **18** (2013) 3098-3107.
- [11] D. Zulli, A. Luongo, Control of primary and subharmonic resonances of a Duffing oscillator via non-linear energy sink, *Int. J. Non-Linear Mechanics* **80** (2016) 170-182.
- [12] B. Yu, A.C.J. Luo, Analytical period-1 motions to chaos in a two-degree-of-freedom oscillator with a hardening nonlinear spring, *Int. J. Dynam. Control* **5** (2017) 436–453.
- [13] M.M. Faith Karahan, M. Pakdemirli, Free and forced vibrations of the strongly nonlinear cubic-quintic Duffing oscillators, *Zeit. Natur. A* **72** (2017) 59-69.
- [14] A. Papangelo, F. Fontanela, A. Grolet, M. Ciavarella, N. Hoffmann, Multistability and localization in forced cyclic structures modelled by weakly-coupled Duffing oscillators, *J. Sound Vibr.* **440** (2019) 202-211.
- [15] J. P. Den Hartog, *Mechanical Vibrations* (4th edition), Dover Publications, New York 1985.
- [16] S. S. Oueini, A. H. Nayfeh and J.R. Pratt, A review of development and implementation of an active nonlinear vibration absorber *Arch. Appl. Mech.*, **69** (1999) 585-620.
- [17] A.H. Nayfeh, *Introduction to Perturbation Techniques*, John Wiley & Sons, 2011.
- [18] A. Okniński and J. Kyzioł, Perturbation analysis of the effective equation for two coupled periodically driven oscillators, *Diff. Eqs. Nonlin. Mec.* **2006** (2006) 56146.
- [19] J. Kyzioł and A. Okniński, Van der Pol-Duffing oscillator: Global view of metamorphoses of the amplitude profiles, *Int. J. Nonlinear Mech.* **116** (2019) 102-106.
- [20] J. Kyzioł and A. Okniński, Exact nonlinear fourth-order equation for two coupled oscillators: metamorphoses of resonance curves, *Acta Phys. Polon. B* **44** (2013) 35-47.
- [21] M. Spivak, *Calculus on Manifolds*, W.A. Benjamin, Inc., Menlo Park (California) 1965.
- [22] C. T. C. Wall, *Singular Points of Plane Curves*, Cambridge University Press, New York 2004.



- [23] J. Kyzioł and A. Okniński, Coupled nonlinear oscillators: metamorphoses of amplitude profiles for the approximate effective equation – the case of 1 : 3 resonance, *Acta Phys. Polon. B* 43 (2012) 1275-1287.
- [24] J. Kyzioł, Metamorphoses of resonance curves for two coupled oscillators: The case of small non-linearities in the main mass frame, *Int. J. Nonlinear Mech.* 76 (2015) 164–168.
- [25] P.J. Holmes, D.A. Rand, The bifurcations of Duffing’s equation: an application of Catastrophe Theory, *Journal of Sound and Vibration* 44 (1976) 237-253.
- [26] J. Kyzioł and A. Okniński, Coupled nonlinear oscillators: metamorphoses of amplitude profiles. The case of the approximate effective equation, *Acta Phys. Polon. B* 42 (2011) 2063-2076.
- [27] J. Awrejcewicz, Modified Poincaré method and implicit function theory, in: *Nonlinear Dynamics: New Theoretical and Applied Results*, J. Awrejcewicz (ed.), Akademie Verlag, Berlin, 1995, pp. 215-229.
- [28] I.M. Gelfand, M.M. Kapranov, A.V. Zelevinsky, *Discriminants, Resultants, and Multidimensional Determinants*, Springer Science & Business Media, 2008.
- [29] S. Janson, Resultant and discriminant of polynomials, Lecture notes, <http://www2.math.uu.se/~protect\char126\relaxsvante/papers/sjN5.pdf>, 2010.
- [30] H.E. Nusse, J.A. Yorke, *Dynamics: Numerical Explorations*, Springer Verlag New York Inc, 1997.